Redox Potential and Peroxide Reactivity of Human Peroxiredoxin 3

ARTICLE *in* BIOCHEMISTRY · JULY 2009

Impact Factor: 3.02 · DOI: 10.1021/bi900558g · Source: PubMed

5 AUTHORS, INCLUDING:

Alexander V Peskin
University of Otago
62 PUBLICATIONS **1,878** CITATIONS
SEE PROFILE

Louise Paton
University of Otago
13 PUBLICATIONS **412** CITATIONS
SEE PROFILE

Christine Winterbourn
University of Otago
363 PUBLICATIONS **19,772** CITATIONS
SEE PROFILE

Mark B Hampton
University of Otago
113 PUBLICATIONS **6,260** CITATIONS
SEE PROFILE

BIOCHEMISTRY
including biophysical chemistry & molecular biology
Article

Biochemistry **2009,** *48,* 6495–6501 6495
DOI: 10.1021/bi900558g

Redox Potential and Peroxide Reactivity of Human Peroxiredoxin 3[†]

Andrew G. Cox, Alexander V. Peskin, Louise N. Paton, Christine C. Winterbourn, and Mark B. Hampton*

Free Radical Research Group and National Research Centre for Growth and Development, Department of Pathology, University of Otago, Christchurch, New Zealand

Received April 2, 2009; Revised Manuscript Received May 21, 2009

ABSTRACT: Peroxiredoxins (Prxs) are a ubiquitous family of thiol peroxidases that protect cells from peroxides and have a putative role in redox signaling. In this study, we investigated the redox properties of human Prx 3, a typical 2-Cys Prx that is localized to the mitochondrial matrix. We found that Prx 3 displayed strong reactivity with H_2O_2, with a competitive kinetic approach generating a second order rate constant of 2×10^7 M^{-1} s^{-1}. This is considerably higher than typical thiols and similar to values for other mammalian 2-Cys Prxs. In contrast, Prx 3 reacted very slowly with the thiol alkylating agents iodoacetamide and *N*-ethylmaleimide. Using dithiothreitol redox buffers, we measured the redox potential of Prx 3 of −290 mV. This is similar to the redox potential of mitochondrial thioredoxin 2 and is consistent with optimal operation of Prx 3 in the mitochondrial matrix.

Peroxiredoxins (Prxs) are a family of thiol peroxidases that decompose H_2O_2 and organic hydroperoxides (*1*). There are six mammalian Prxs that are classified into three subtypes (typical 2-Cys, atypical 2-Cys, and typical 1-Cys) depending on their catalytic mechanism of H_2O_2 reduction (*2*). The typical 2-Cys Prxs are highly abundant enzymes, distributed in various compartments including the cytosol (Prx 1 and 2), mitochondria (Prx 3), and the endoplasmic reticulum (Prx 4). Typical 2-Cys Prxs contain a peroxidatic cysteine residue in the active site that is oxidized by hydroperoxides to form a sulfenic acid. The sulfenic acid condenses with the resolving cysteine of an adjacent Prx to form a disulfide-linked dimer reducible by thioredoxin. In addition to the basic catalytic cycle, the sulfenic acid intermediate can be hyperoxidized to form a sulfinic acid that is catalytically inactive. This switch is proposed to play an integral role in these proteins acting as redox sensors that control the cellular response to oxidative stress (*3*).

The catalytic interconversion of Prx redox states in biological systems will be dependent on the local environment including peroxide fluxes, reductant concentrations, regulatory binding proteins, and the innate biochemical properties of the individual Prxs. There is limited information available on the enzymatic properties of Prx 3, but differences from other members of the Prx family are expected. Prx 3 functions in the mitochondrial matrix and is reduced by mitochondrial-specific thioredoxin and thioredoxin reductase. Mitochondria are the major source of cellular reactive oxygen species (ROS), accounting for up to 90% of the total production (*4*). Most mitochondrial-derived ROS are produced during aerobic respiration as electrons leak from respiratory complexes I and III to form superoxide (*4*). There is increasing evidence that the mitochondrial redox environment is regulated independently of the cytosol (*5*). We have previously shown that Prx 3 is oxidized by apoptosis inducers (*6*, *7*) and thioredoxin reductase inhibitors (*8*) without effects on cytoplasmic Prxs.

The aim of this study was to measure kinetic parameters of human Prx 3 that would enable the prediction of Prx 3 activity in the mitochondrial environment. Competitive kinetic approaches have revealed that many Prxs react with H_2O_2 at rates comparable to that of catalase ($\sim10^7$ M^{-1} s^{-1}) (*9*−*12*). However, there have been no kinetic studies examining the reactivity of Prx 3 with H_2O_2. During the catalytic breakdown of H_2O_2, the peroxidatic cysteine can be hyperoxidized to a sulfinic acid (1 per 1,300 turnovers for Prx 1) (*13*). We have observed Prx 3 to be less susceptible to hyperoxidation than Prx 1 and Prx 2 (*14*). One explanation would be slower turnover due to decreased reactivity of Prx 3. The redox midpoint potential for the peroxiredoxin active site dithiol has been extensively studied in plants yielding values between −288 and −325 mV (*15*−*17*). Recently, the redox potential of the bacterial 2-Cys peroxiredoxin AhpC was determined to be −178 mV, considerably more positive than the chloroplast Prxs (*12*). There are no reports for the midpoint potential of any mammalian peroxiredoxin. However, the redox potentials of the physiological electron donors thioredoxin 1, present in cytoplasm, and thioredoxin 2, localized to mitochondria, have been determined to be −230 and −292 mV respectively (*18*, *19*). In the present study, we determined the redox potential of Prx 3 and investigated its reactivity with H_2O_2 and alkylating agents.

MATERIALS AND METHODS

Materials. Recombinant human Prx 3, without the mitochondrial leader sequence, was from Young and Abfrontier

[†]This project was supported by the Royal Society Marsden Fund and the National Research Centre for Growth and Development. A.G.C. is a recipient of a Top Achiever Doctoral Scholarship from the Tertiary Education Commission.

*Corresponding author. Phone: (64 3) 378 6225. Fax: (64 3) 364 1083. E-mail: mark.hampton@otago.ac.nz.

 Published on Web 05/22/2009

(Seoul, Korea). DL-Dithiothreitol (DTT), *trans*-4,5-dihydroxy-1,2-dithiane (oxidized DTT), *N*-ethylmaleimide (NEM), and iodoacetamide (IAM) were from Sigma-Aldrich (St Louis, MO). Catalase derived from bovine liver and human erythrocytes was from Sigma-Aldrich (St Louis, MO). Micro Bio-Spin 6 chromotography columns, acrylamide, and Bio-Rad DC protein assays were purchased from Bio-Rad (Hercules, CA). H_2O_2 was from BDH (Poole, UK). All other chemicals and reagents were from Sigma-Aldrich (St Louis, MO) and BDH laboratory Supplies (Poole, UK). All water was deionized and filtered using a Milli-Q filtration system.

H_2O_2 and Protein Quantification. The concentration of H_2O_2 solutions was measured at 240 nm (ε_{240}=43.6 M^{-1} cm^{-1}). Folin−Lowry protein assays were performed on the commercially obtained proteins prior to investigation. The protein concentration for Prx 3 was determined by the absorption at 280 nm (ε_{280}=19,420 M^{-1} cm^{-1}) (personal communication with Daniel Shin, Young and Frontier Co. Ltd.). The protein concentration of HRP was determined by absorption at 403 nm ($\varepsilon_{403}=1.02 \times 10^5$ M^{-1} cm^{-1}) (*10*).

Peroxiredoxin 3 Thiol Reduction. Prx 3 was reduced with 25 mM DTT for 30 min in 100 mM potassium phosphate buffer at pH 7.4 containing 10 μg/mL bovine catalase and passed through a Micro Bio-Gel 6 spin column (Bio-Rad, Hercules, CA). If some oxidation was detected, we used a Micro Bio-Gel 6 spin column that had been pre-equilibrated with buffer containing 10 μg/mL bovine catalase followed by buffer alone to remove any trace of catalase remaining. Reduced Prx 3 in the presence of 1% SDS had three free thiols as determined by reaction with DTNB (ε_{412}=14,200 M^{-1} cm^{-1}).

Competition Reactions with Catalase. Reduced Prx 3 (5 μM) was treated with 5 μM H_2O_2 in the presence of various concentrations of bovine or human catalase at 20 °C for 5 min. Reactions were quenched with 50 mM NEM in sample buffer containing 2% SDS, 10% glycerol, and 62.5 mM Tris at pH 6.8. Samples run under nonreducing conditions on 15% SDS−PAGE ran either as a reduced monomer (~21 kDa) or a reversibly oxidized dimer (~42 kDa). Proteins were detected by Coomassie or silver stain. Stained gels were scanned using a Fluor-S Multi-Imager (Bio-Rad, Hercules, CA). Images were analyzed using Quantity One software (Bio-Rad, Hercules, CA).

Competition Kinetics with Horseradish Peroxidase (HRP). The second order rate constant for the reaction of Prx 3 with H_2O_2 was determined by a competitive approach using horseradish peroxidase (HRP) (*10*). HRP is rapidly converted by H_2O_2 to compound I ($k = 1.7 \times 10^7$ M^{-1} s^{-1}), which can be monitored at 403 nm. In the presence of increasing concentrations of reduced Prx 3, the amount of HRP converted to compound I by H_2O_2 is diminished as Prx 3 competes for the substrate. Knowing the initial concentrations of HRP and Prx 3 as well as the rate at which HRP reacts with H_2O_2, we can determine the rate at which Prx 3 reacts with H_2O_2. Initial concentrations of H_2O_2, HRP, and Prx 3 were determined spectrophotometrically as described above. Twenty micromolar HRP was treated with 10 μM H_2O_2 in the presence of prereduced Prx 3 (7−28 μM). Spectra were measured within 10 s of mixing using a NanoDrop spectrophotometer (BioLab Nanodrop Technologies, Wilmington, DE). The fractional inhibition of HRP oxidation at different concentrations of Prx 3 was used to obtain the second order rate constant for Prx 3. In experiments to investigate the pH dependence of the competition reaction, a BPACE buffer was used (10 mM sodium phosphate, 10 mM sodium citrate, 10 mM boric acid, 1 mM EDTA, and 100 mM ammonium sulfate with the pH adjusted with ammonium hydroxide or sulfuric acid (*20*)).

Mass Spectrometry Analysis of Prx 3 Alkylation by Direct Infusion. Reduced Prx 3 (10 μM) was treated with IAM or NEM for 30 min before being desalted in a Micro Bio-Gel 6 spin column equilibrated with water. The desalted protein was diluted 1:1 with acetonitrile containing 0.1% formic acid. Mass spectrometry was performed using a LCQ DECA XPplus ion trap instrument (ThermoFinnigan, San Jose, CA). Samples were directly infused using a Hamilton syringe at a flow rate of 5 μL/min. A full scan for the mass range 100−2000 m/z was monitored. Data were collected for 1 min before deconvolution using BioworksBrowser 3.1 SR1 (ThermoFinnigan).

Mass Spectrometry Analysis of Chymotrypic Digests of Alkylated Prx 3. Reduced Prx 3 (10 μM) was treated with IAM (100 μM−100 mM) or NEM (1 μM−1 mM) for 30 min before being desalted in a Micro Bio-Gel 6 spin column equilibrated with 100 mM Tris-HCl and 10 mM $CaCl_2$ at pH 7.8. Sequencing grade chymotrypsin (Roche, Mannheim, Germany) was prepared at a concentration of 1 mg/mL in 1 mM HCl and was added to Prx 3 samples at a ratio of 1:60. Samples were incubated for 12 h with chymotrypsin before being reduced with immobilized TCEP disulfide reducing gel (Pierce, Rockford, IL) according to the manufacturer's instructions. Formic acid was added to a final concentration of 0.1% w/w, and samples were placed in glass vials for automated LC-MS analysis. Peptides were analyzed using a Finnigan LCQDeca ion trap mass spectrometer equipped with a Surveyor HPLC system and a Jupiter 4u Proteo 90A column (150 × 2 mm) (Phenomenex, CA). Liquid chromatography was carried out at ambient temperature at a flow rate of 200 μL/min. The solvent system consisted of a linear gradient over 60 min from 95% solvent A (0.1% formic acid in water) and 5% solvent B (0.1% formic acid in acetonitrile) to 5% solvent A and 95% solvent B, followed by a 15 min wash period using 5% solvent A and 95% solvent B. LC-MS data were processed using Qual Browser v1.3.

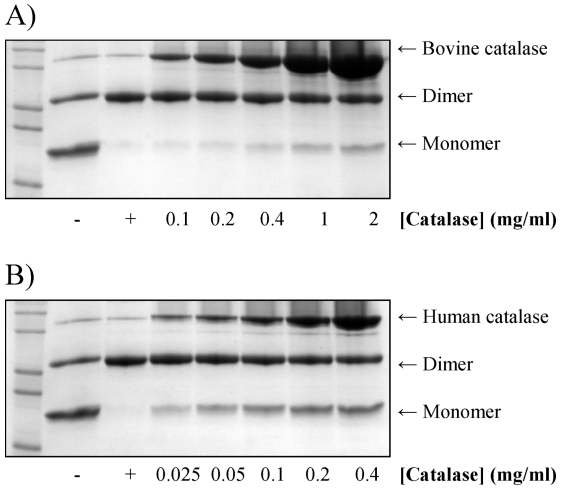

FIGURE 1: Reactivity of Prx-3 with H_2O_2. Competition with catalase. Reduced Prx 3 (5 μM) was reacted with 5 μM H_2O_2 in the presence of increasing amounts of bovine (A) or human (B) catalase. After 2 min, the reaction was quenched by the addition of sample buffer containing 50 mM NEM. Samples were resolved by SDS−PAGE in nonreducing conditions and Coomassie stained. (−) control in the absence of H_2O_2; (+) control in the presence of H_2O_2. Gels are representative of 3 independent experiments.

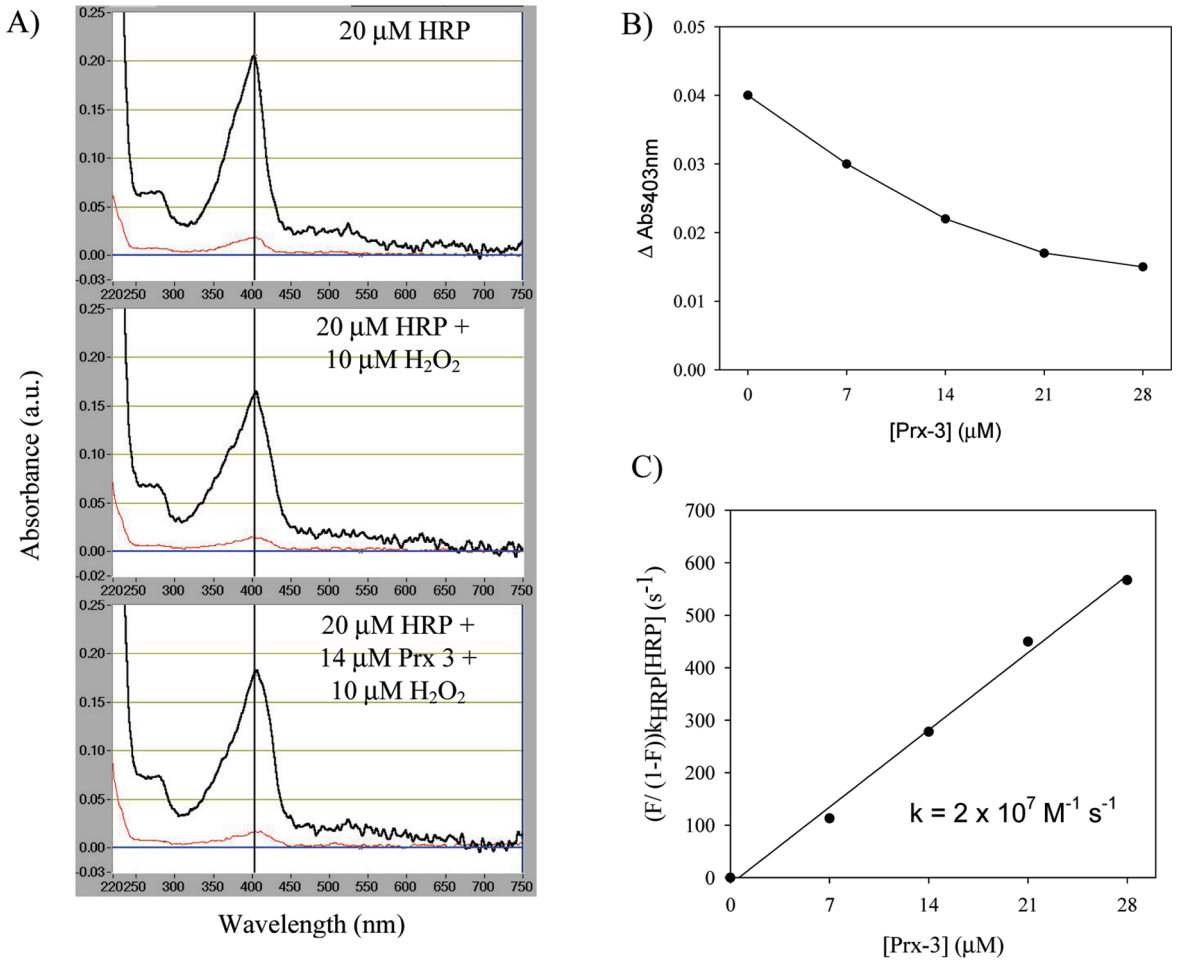

FIGURE 2: Determination of the second order rate constant for the reaction of Prx-3 with H_2O_2 by competition with HRP. Reaction mixtures containing 20 μM HRP and 7−28 μM Prx 3 were treated with 10 μM H_2O_2. Spectra were recorded after 10 s using a NanoDrop spectrophotometer with a 1-mm path length (A). The change in absorbance at 403 nm was measured (B) and used to calculate the fractional inhibition (F) of HRP oxidation at each Prx 3 concentration (C) enabling the determination of the rate constant.

Time Course of Prx 3 Alkylation. Reduced Prx 3 (5 μM) was treated with 10 mM IAM or 100 μM NEM for various times before the reaction was quenched by the addition of 10 μM H_2O_2 to oxidize remaining reactive thiols. Samples were subsequently placed in nonreducing sample buffer containing 200 mM IAM or NEM and resolved by SDS−PAGE. Excess IAM or NEM were used in the sample buffer to ensure that all thiols including the nonactive site cysteine were fully alkylated. Proteins were detected by silver stain. Stained gels were scanned using Fluor-S MultiImager (Bio-Rad, Hercules, CA). Images were analyzed using Quantity One software (Bio-Rad, Hercules, CA).

Determination of the Redox Potential. The redox potential of Prx 3 was determined by redox titrations with the reduced and oxidized forms of DTT using an adapted method previously described (*21*). Prx 3 (7 μM) was added to aliquots of 100 mM potassium phosphate and 1 mM EDTA at pH 7, containing various amounts of reduced and oxidized DTT to achieve defined E_h values (to a total DTT concentration of 2 mM). The E_h values of the various DTT buffers were determined according to the Nernst equation ($E_h = E_0 + 2.3 \times RT/nF \times \log([DTT_{ox}]/[DTT_{red}])$), where $E_0 = -330$ mV at pH 7, and $n = 2$. Prx 3 was allowed to equilibrate at room temperature for 2 h before the reaction was quenched by the addition of sample buffer (2% SDS, 10% glycerol, and 62.5 mM Tris at pH 6.8) containing 50 mM NEM and run on 15% SDS−PAGE as described above.

Statistics. Values are shown as the mean and standard error of three or more independent experiments, and all gels and kinetic values are representative of at least three independent experiments. Statistical analyses were performed with the software package SigmaStat (Systat, San Rafael, CA, USA).

RESULTS

Reactivity of Prx 3 with H_2O_2. To investigate the reactivity of Prx 3 toward H_2O_2, we monitored the oxidation of Prx 3 in the presence of increasing amounts of bovine (Figure 1A) or human catalase (Figure 1B). The oxidation of Prx 3 was determined by monitoring the conversion of reduced monomer to oxidized dimer on nonreducing SDS−PAGE. High concentrations of catalase were required to inhibit the reaction. Bovine catalase, which has a rate constant of 6×10^6 M^{-1} s^{-1}, was less effective than human catalase, which has a rate constant of 3×10^7 M^{-1} s^{-1} (*22*). The catalase inhibition suggests that Prx 3 reacts with H_2O_2 at a rate in the order of 10^7 M^{-1} s^{-1}.

To obtain a more accurate rate constant, we used a competitive kinetic approach with HRP, which reacts with H_2O_2 with a rate constant of 1.7×10^7 M^{-1} s^{-1} to form compound I that can be measured at 403 nm (Figure 2A). Prx 3 inhibited compound I formation in a dose-dependent manner (Figure 2B). For each concentration of Prx 3, the fractional inhibition (F) was determined and used to construct a plot of $(F/(1 - F))k_{HRP}[HRP]$ versus [Prx 3] (Figure 2C). The slope of this line was used to

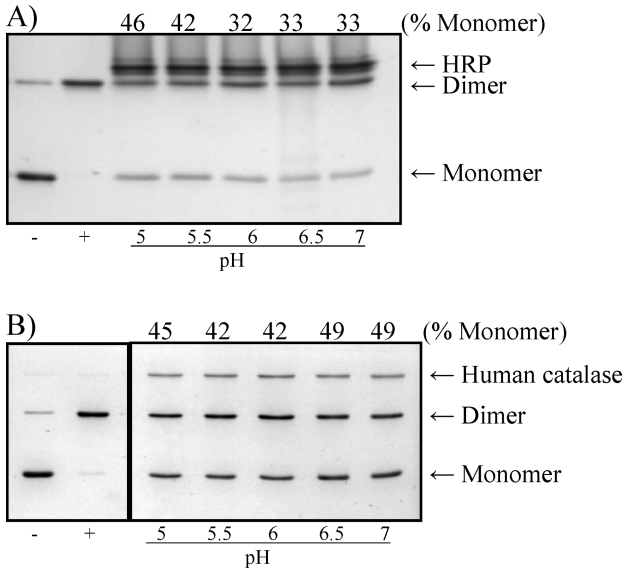

FIGURE 3: Competition reactions between Prx 3 and HRP or human catalase at different pH. (A) HRP (50 μM) and reduced Prx 3 (50 μM) were diluted 10-fold into BPACE buffer (10 mM sodium phosphate, 10 mM sodium citrate, 10 mM boric acid, 1 mM EDTA, and 100 mM ammonium sulfate) at different pH. (B) Reduced Prx 3 (50 μM) was diluted 10-fold into BPACE buffer containing 0.1 mg/mL human catalase. Note that there is a solid line in the gel representing lanes that have been removed. The reaction was started by the addition of 5 μM H_2O_2 and was quenched after 2 min by adding nonreducing sample buffer containing 50 mM NEM. Samples were resolved by SDS−PAGE and silver stained. (−) control in the absence of H_2O_2; (+) control in the presence of H_2O_2. Gels are representative of 3 independent experiments.

calculate a second order rate constant for the reaction between Prx 3 and H_2O_2 of 2×10^7 M^{-1} s^{-1}.

The pH dependence of the reaction between Prx 3 and H_2O_2 in competition with HRP and human catalase was monitored. HRP and catalase react with H_2O_2 in a pH-independent manner above pH 5 (*10*, *22*). Prx 3 competed effectively for H_2O_2 in the presence of either HRP or catalase at all measured pH values, with only a subtle increase in the proportion of reduced Prx 3 in the HRP system (Figure 3A), indicating that the peroxidatic thiol of Prx 3 has a pK_a well below 7. Attempts to accurately quantify this value are restricted by impairment of HRP and catalase activity at lower pH values.

Reactivity of Prx 3 toward Thiol Alkylating Agents. To investigate whether the high reactivity of Prx 3 with H_2O_2 is reflected in reactivity toward the thiol reagents, reduced Prx 3 (10 μM) was alkylated with various doses of IAM (1−100 mM) or NEM (10 μM−1 mM) for 30 min before being desalted and analyzed by mass spectrometry. Prx 3 was only partially alkylated at one site with 1 mM IAM (+57 mass units); however, with 10 or 100 mM IAM two sites were modified (+114 mass units) (Figure 4A). Lower doses of NEM (10 μM) were required for partial alkylation of two sites (+125 mass units, +250 mass units), with complete modification of two sites at 100 μM or 1 mM NEM (+250 mass units) (Figure 4B). Analysis of chymotryptic digests by LC-MS revealed that IAM preferentially modified the peroxidatic cysteine (C107), closely followed by the resolving cysteine (C229) (Table 1). NEM reacted to a similar extent with both the peroxidatic and resolving cysteines. The third cysteine (C126), which is not involved in catalysis, only became modified with the highest dose of each thiol reagent. All three cysteine residues were modified following incubation with either 100 mM IAM or 100 mM NEM for 1 h in the presence of 1% SDS (data not shown).

Having shown that Prx 3 was alkylated primarily at the peroxidatic and resolving cysteines, we used SDS−PAGE under nonreducing conditions to estimate the global rate of alkylation. Alkylated Prx 3 is unable to dimerize following the addition of H_2O_2 and therefore migrates as the monomer. The accumulation of monomer was followed with either 10 mM IAM over 120 min or 100 μM NEM over 20 min (Figure 5). It is clear from the time course data that the catalytic cysteines of Prx 3 react very slowly with IAM and NEM over several minutes (NEM) or hours (IAM). From these blots, values for the rate of reaction were estimated to be 1×10^{-3} h^{-1} and 1 h^{-1} for IAM and NEM, respectively, which takes into account that two peroxidatic cysteines have to be alkylated to prevent dimer formation. Assuming a second order reaction, rate constants would be less than 0.1 M^{-1} s^{-1} and 100 M^{-1} s^{-1}, for IAM and NEM, respectively, highlighting the relative resistance of Prx 3 to alkylation compared to H_2O_2.

Determination of the Midpoint Redox Potential of Prx 3. Given that Prx 3 operates in the redox environment of the mitochondria, we suspected that Prx 3 might exhibit a redox potential appropriate for this environment. Prx 3 was equilibrated in either its oxidized or reduced form in 2 mM DTT_{red}/DTT_{ox} buffers over a range of redox potentials (−330 to −250 mV). Following a 2 h equilibration period, the reaction was quenched by the addition of nonreducing sample buffer containing 50 mM NEM. The samples were run on SDS−PAGE in nonreducing conditions in order to monitor the amounts of reduced monomer and oxidized dimer (Figure 6A). Using this nonreducing gel approach, we determined the midpoint redox potential to be −290 mV (Figure 6B). Similar results were obtained when the protein was equilibrated for longer periods in 10 mM DTT_{red}/DTT_{ox} buffers (data not shown).

DISCUSSION

In the current study, we have determined that mitochondrial Prx 3 has an extremely high reactivity with H_2O_2, with a rate constant of 2×10^7 M^{-1} s^{-1}. This is considerably higher than any reported thiol protein, excluding other members of the Prx family. An increasing number of studies have revealed that many Prxs from bacteria (AhpC) (*12*), yeast (Tpx 1 and Tpx 2) (*10*), and humans (Prx 2) (*11*, *23*) react with H_2O_2 at rates comparable to those of the specialized heme and selenocysteine proteins catalase and glutathione peroxidase (10^7−10^8 M^{-1} s^{-1}). Calculation of these rate constants is dependent on competitive enzyme kinetics. One potential complication of the HRP competition assay is if the reduced thiols of Prx 3 were able to convert HRP compound I to compound II (*24*). However, we can exclude this having a significant effect in this study because the HRP absorbances in Figure 2, measured at 10 s, were unchanged after a further 30 s even though residual reduced Prx 3 was present. Under our conditions, compound I was stable over the period of analysis (data not shown). If anything, these assumptions would only lead to an underestimation of the rate of reaction between Prx 3 and H_2O_2.

The alkylation studies showed that IAM and NEM are particularly slow in reacting with Prx 3, with the reaction 10^6−10^9 times slower than the reaction with H_2O_2. The peroxidatic and resolving cysteines were the major targets, while the third cysteine of Prx 3 was resistant to alkylation, which may indicate limited access to this cysteine. The reaction of IAM with Prx 3

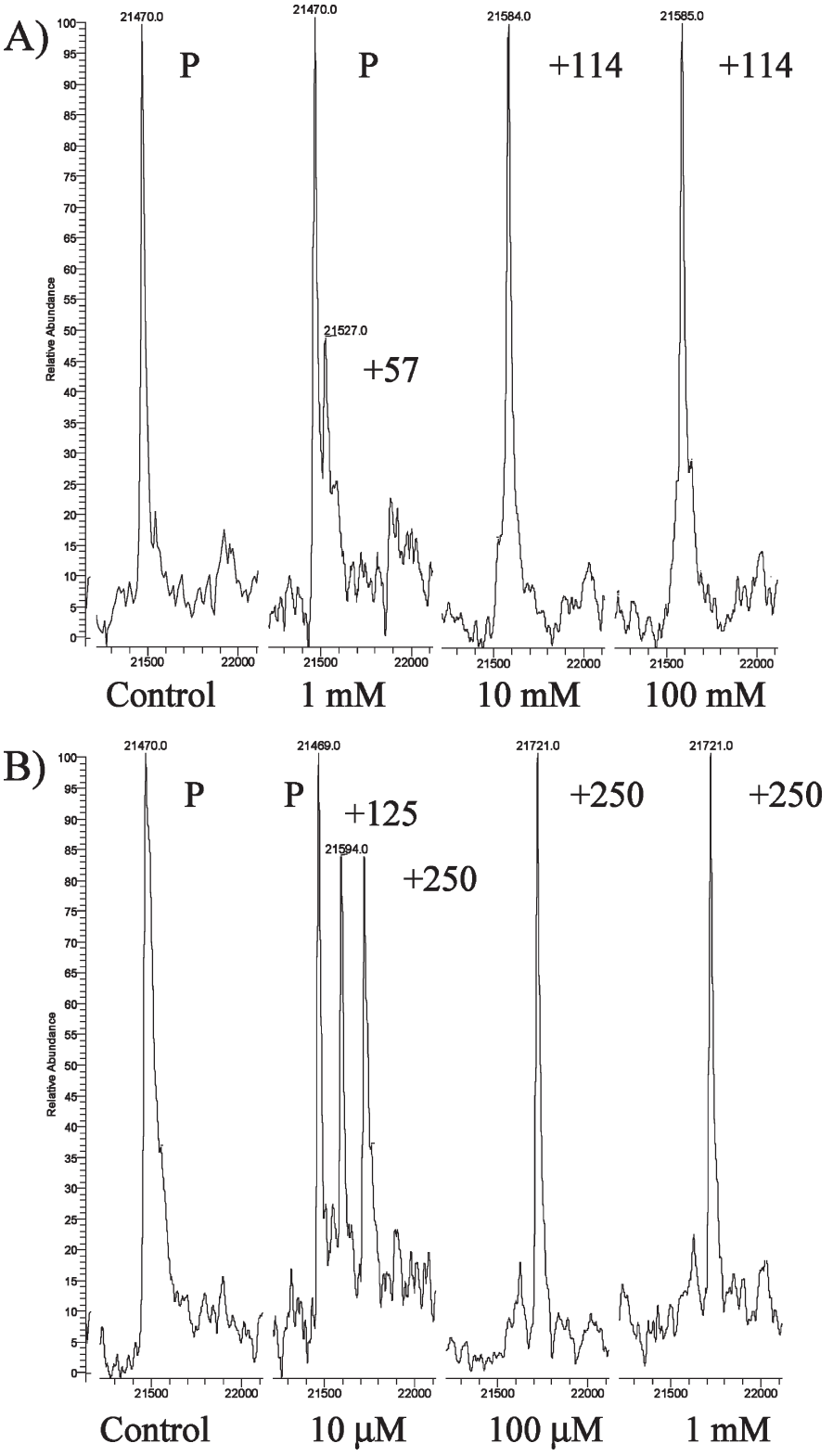

FIGURE 4: Mass spectrometry analysis of IAM and NEM alkylated Prx-3. Reduced Prx 3 (10 μM) was reacted with increasing concentrations of either IAM (A) or NEM (B) for 30 min before samples were desalted and analyzed by mass spectrometry using an LCQ DECA XPplus ion trap instrument (ThermoFinnigan, San Jose, CA). P, parent protein with a m/z ratio of 21,470. For the alkylation of Prx 3 with IAM, +57, one alkylated site, and + 114, two alkylated sites. For the alkylation of Prx 3 with NEM, +125, one alkylated site, and +250, two alkylated sites.

was approximately 10^2-10^3 times slower than that with other redox-active protein thiols such as thioredoxin, glyceraldehyde-3-phosphate dehydrogenase, or protein disulfide isomerase (*25*−*27*). It is clear that with a low K_m for H_2O_2, the Prx active site is constructed to rapidly react with peroxide substrates over thiol reactive agents (*11*, *20*). The low reactivity of Prxs with NEM explains why very high concentrations (100 mM) are required for efficient alkylation in cellular studies (*6*−*8*).

Prx 3 appears to have a very low redox potential ($E_0 = -290$ mV) that is closely matched to the redox potential of its physiological electron donor, mitochondrial thioredoxin 2 ($E_0 = -292$ mV) (*19*). The proximity of these redox potentials

Table 1: Peptide Adducts Detected by LC-MS in Chymotryptic Digest of Alkylated Prx 3[a]

			IAM (mM)				NEM (mM)			
alkylated cysteine containing peptide	alkylation	expected mass (MH+)	0.1	1	10	100	0.001	0.01	0.1	1
VCPTEIVAF (C107)	control	978.5 1+								
	IAM	1035.5 1+	+	++	+++	+++	+	++	+++	+++
	NEM	1103.5 1+								
HDVNCEVVAVSVDSHF (C126)	control	1756.8 1+								
	IAM	1813.8 1+	−	−	−	+	−	−	−	+
	NEM	1881.8 1+								
VETHGEVCPANW (C229)	control	1341.6 1+								
	IAM	1398.6 1+	−	+	+++	+++	−	++	+++	+++
	NEM	1466.6 1+								

[a] (−) Not detected, (+) minor peak, (++) major peak, (+++) highest amount of alkylated product.

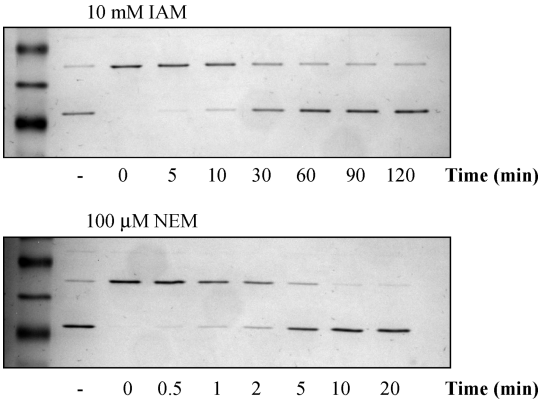

FIGURE 5: Time course of Prx 3 alkylation with IAM and NEM. Reduced Prx 3 (5 μM) was treated with IAM (10 mM) or NEM (100 μM) for various times before the reaction was quenched with H_2O_2 (10 μM). Samples were resolved by SDS−PAGE in nonreducing conditions and silver stained. (−) control in the absence of H_2O_2. Gels are representative of 3 independent experiments.

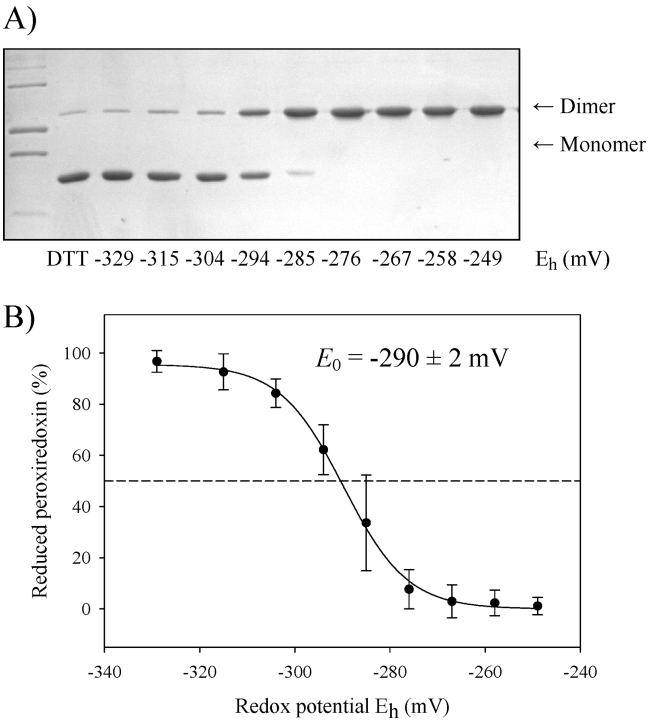

FIGURE 6: Redox potential of Prx-3. Prx 3 (7 μM) was added to redox buffers containing different ratios of DTT_{red}/DTT_{ox}. The samples were left to equilibrate for 2 h before the reaction was quenched by the addition of sample buffer containing 50 mM NEM. Samples were run on SDS−PAGE in nonreducing conditions and Coomassie stained (A). The amount of oxidized and reduced Prx 3 was determined by densitometry (B), plotted against E_h, and fitted with an exponential curve to calculate the E_0. Data points represent the mean ± the SE of 3 independent experiments.

leads to the prospect that Prx 3 could reduce oxidized thioredoxin 2, depending on kinetic factors such as interaction of thioredoxin 2 with the dimer (oxidized) or dodecamer (reduced) forms of Prx 3 (*9*). This intriguing possibility warrants further study. The redox potential is at least 50 mV more negative than thioredoxin 1 (E_0 = −230 mV) (*18*), glutathione (E_0 = −240 mV) (*28*), glutaredoxin 1 (E_0 = −232 mV), and glutaredoxin 2 (E_0 = −221 mV) (*29*), providing a thermodynamic barrier to reduction by these alternative electron donors. Lipoic acid is present at a considerable concentration in the mitochondria, where it can be reduced by either dihydrolipoamide dehydrogenase or thioredoxin reductase (*30*). Interestingly, the redox potential of the dihydrolipoic acid/lipoic acid couple (E_0 = −290 mV) (*31*) makes dihydrolipoic acid well poised to be an electron donor to Prx 3. Indeed, previous studies have shown that dihydrolipoic acid is a potent reductant for thioredoxin 1 and bovine 1-Cys Prx (*32*, *33*). Studies have also shown that the 2-Cys Prxs bind and can be reduced by cyclophilin A (*34*, *35*). Cyclophilin A is a cytoplasmic enzyme; however, the mitochondrial isoform cyclophilin D may capable of being an alternative electron donor to Prx 3. With this in mind, it is noteworthy that the midpoint redox potential of a plant cyclophilin, cyp20−3, was recently determined to be −319 mV (*36*). There is clearly a need for further studies investigating the physiological relevance of such interactions.

Mitochondria contain both Prx 3 and the atypical 2-Cys Prx 5, which is broadly distributed between several cellular compartments. In mitochondria, Prx 5 is ~3-fold less abundant than Prx 3 (*37*). In vitro kinetic studies have revealed that Prx 5 functions most efficiently as a peroxynitrite reductase, exhibiting a rate constant of 10^7 M^{-1} s^{-1} for reaction with peroxynitrite, compared to 10^5 M^{-1} s^{-1} for H_2O_2 (*38*). Thus, Prx 3 has much higher reactivity with H_2O_2. The rate of reaction of Prx 3 with peroxynitrite has not been measured, but if it behaves similarly to Prx 2 (*23*), the rate constant would be expected to be ~10-fold less than that for H_2O_2. Therefore, the kinetic properties of the mitochondrial Prxs suggest that these enzymes may have nonredundant roles in antioxidant defense, with Prx 3 preferentially decomposing H_2O_2 and Prx 5 being more effective against peroxynitrite (*38*). A prevailing view was that glutathione peroxidase 1 is the major H_2O_2 catabolizing enzyme in the mitochondrial matrix; however, its peroxidase activity could only

account for 15% of the total H_2O_2 production (*39*). The abundance of Prx 3 in mitochondria (*14*, *40*) coupled with the reactivity toward H_2O_2 shown here suggests that Prx 3 is more likely to perform this function.

REFERENCES

(1) Rhee, S. G., Chae, H. Z., and Kim, K. (2005) Peroxiredoxins: A historical overview and speculative preview of novel mechanisms and emerging concepts in cell signaling. *Free Radical Biol. Med. 38*, 1543–1552.

(2) Wood, Z. A., Schroder, E., Harris, J. R., and Poole, L. B. (2003) Structure, mechanism and regulation of peroxiredoxins. *Trends Biochem. Sci. 28*, 32–40.

(3) Wood, Z. A., Poole, L. B., and Karplus, P. A. (2003) Peroxiredoxin evolution and the regulation of hydrogen peroxide signaling. *Science 300*, 650–653.

(4) Murphy, M. P. (2009) How mitochondria produce reactive oxygen species. *Biochem. J. 417*, 1–13.

(5) Go, Y. M., and Jones, D. P. (2008) Redox compartmentalization in eukaryotic cells. *Biochim. Biophys. Acta 1780*, 1273–1290.

(6) Cox, A. G., Pullar, J. M., Hughes, G., Ledgerwood, E. C., and Hampton, M. B. (2008) Oxidation of mitochondrial peroxiredoxin 3 during the initiation of receptor-mediated apoptosis. *Free Radical Biol. Med. 44*, 1001–1009.

(7) Brown, K. K., Eriksson, S. E., Arner, E. S., and Hampton, M. B. (2008) Mitochondrial peroxiredoxin 3 is rapidly oxidized in cells treated with isothiocyanates. *Free Radical Biol. Med. 45*, 494–502.

(8) Cox, A. G., Brown, K. K., Arner, E. S., and Hampton, M. B. (2008) The thioredoxin reductase inhibitor auranofin triggers apoptosis through a Bax/Bak-dependent process that involves peroxiredoxin 3 oxidation. *Biochem. Pharmacol. 76*, 1097–1109.

(9) Parsonage, D., Youngblood, D. S., Sarma, G. N., Wood, Z. A., Karplus, P. A., and Poole, L. B. (2005) Analysis of the link between enzymatic activity and oligomeric state in AhpC, a bacterial peroxiredoxin. *Biochemistry 44*, 10583–10592.

(10) Ogusucu, R., Rettori, D., Munhoz, D. C., Netto, L. E., and Augusto, O. (2007) Reactions of yeast thioredoxin peroxidases I and II with hydrogen peroxide and peroxynitrite: rate constants by competitive kinetics. *Free Radical Biol. Med. 42*, 326–334.

(11) Peskin, A. V., Low, F. M., Paton, L. N., Maghzal, G. J., Hampton, M. B., and Winterbourn, C. C. (2007) The high reactivity peroxiredoxin 2 with H_2O_2 is not reflected in its reaction with other oxidants and thiol reagents. *J. Biol. Chem. 282*, 11885–11892.

(12) Parsonage, D., Karplus, P. A., and Poole, L. B. (2008) Substrate specificity and redox potential of AhpC, a bacterial peroxiredoxin. *Proc. Natl. Acad. Sci. U.S.A. 105*, 8209–8214.

(13) Yang, K. S., Kang, S. W., Woo, H. A., Hwang, S. C., Chae, H. Z., Kim, K., and Rhee, S. G. (2002) Inactivation of human peroxiredoxin I during catalysis as the result of the oxidation of the catalytic site cysteine to cysteine-sulfinic acid. *J. Biol. Chem. 277*, 38029–38036.

(14) Cox, A. G., Pearson, A. G., Pullar, J. M., Jönsson, T. J., Lowther, W. T., Winterbourn, C. C., and Hampton, M. B. (2009) Mitochondrial peroxiredoxin 3 is more resilient to hyperoxidation than cytoplasmic peroxiredoxins. *Biochem. J. 421*, 51–58.

(15) Konig, J., Baier, M., Horling, F., Kahmann, U., Harris, G., Schurmann, P., and Dietz, K. J. (2002) The plant-specific function of 2-Cys peroxiredoxin-mediated detoxification of peroxides in the redox-hierarchy of photosynthetic electron flux. *Proc. Natl. Acad. Sci. U.S.A. 99*, 5738–5743.

(16) Rouhier, N., Gelhaye, E., Gualberto, J. M., Jordy, M. N., De Fay, E., Hirasawa, M., Duplessis, S., Lemaire, S. D., Frey, P., Martin, F., Manieri, W., Knaff, D. B., and Jacquot, J. P. (2004) Poplar peroxiredoxin Q. A thioredoxin-linked chloroplast antioxidant functional in pathogen defense. *Plant Physiol. 134*, 1027–1038.

(17) Dietz, K. J. (2007) The dual function of plant peroxiredoxins in antioxidant defence and redox signaling. *Subcell Biochem. 44*, 267–294.

(18) Watson, W. H., Pohl, J., Montfort, W. R., Stuchlik, O., Reed, M. S., Powis, G., and Jones, D. P. (2003) Redox potential of human thioredoxin 1 and identification of a second dithiol/disulfide motif. *J. Biol. Chem. 278*, 33408–33415.

(19) Halvey, P. J., Watson, W. H., Hansen, J. M., Go, Y. M., Samali, A., and Jones, D. P. (2005) Compartmental oxidation of thiol-disulphide redox couples during epidermal growth factor signalling. *Biochem. J. 386*, 215–219.

(20) Nelson, K. J., Parsonage, D., Hall, A., Karplus, P. A., and Poole, L. B. (2008) Cysteine pKa values for the bacterial peroxiredoxin AhpC. *Biochemistry 47*, 12860–12868.

(21) Hirasawa, M., Schurmann, P., Jacquot, J. P., Manieri, W., Jacquot, P., Keryer, E., Hartman, F. C., and Knaff, D. B. (1999) Oxidation-reduction properties of chloroplast thioredoxins, ferredoxin:thioredoxin reductase, and thioredoxin f-regulated enzymes. *Biochemistry 38*, 5200–5205.

(22) Dunford, H. B. (1999) Heme Peroxidases , Wiley-VCH, Weinheim, Germany.

(23) Manta, B., Hugo, M., Ortiz, C., Ferrer-Sueta, G., Trujillo, M., and Denicola, A. (2009) The peroxidase and peroxynitrite reductase activity of human erythrocyte peroxiredoxin 2. *Arch. Biochem. Biophys. 484*, 146–154.

(24) Trujillo, M., Ferrer-Sueta, G., and Radi, R. (2008) Kinetic studies on peroxynitrite reduction by peroxiredoxins. *Methods Enzymol. 441*, 173–196.

(25) Kallis, G. B., and Holmgren, A. (1980) Differential reactivity of the functional sulfhydryl groups of cysteine-32 and cysteine-35 present in the reduced form of thioredoxin from *Escherichia coli*. *J. Biol. Chem. 255*, 10261–10265.

(26) Marchal, S., and Branlant, G. (1999) Evidence for the chemical activation of essential cys-302 upon cofactor binding to nonphosphorylating glyceraldehyde 3-phosphate dehydrogenase from Streptococcus mutans. *Biochemistry 38*, 12950–12958.

(27) Hawkins, H. C., de Nardi, M., and Freedman, R. B. (1991) Redox properties and cross-linking of the dithiol/disulphide active sites of mammalian protein disulphide-isomerase. *Biochem. J. 275* (Pt 2), 341–348.

(28) Aslund, F., Berndt, K. D., and Holmgren, A. (1997) Redox potentials of glutaredoxins and other thiol-disulfide oxidoreductases of the thioredoxin superfamily determined by direct protein-protein redox equilibria. *J. Biol. Chem. 272*, 30780–30786.

(29) Sagemark, J., Elgan, T. H., Burglin, T. R., Johansson, C., Holmgren, A., and Berndt, K. D. (2007) Redox properties and evolution of human glutaredoxins. *Proteins 68*, 879–892.

(30) Moini, H., Packer, L., and Saris, N. E. (2002) Antioxidant and prooxidant activities of alpha-lipoic acid and dihydrolipoic acid. *Toxicol. Appl. Pharmacol. 182*, 84–90.

(31) Lamoureux, G. V., and Whitesides, G. M. (1993) Synthesis of dithiols as reducing agents for disulfides ini neutral aqueous solution and comparison of reduction potentials. *J. Org. Chem. 58*, 633–641.

(32) Packer, L., Witt, E. H., and Tritschler, H. J. (1995) α-Lipoic acid as a biological antioxidant. *Free Radical Biol. Med. 19*, 227–250.

(33) Peshenko, I. V., and Shichi, H. (2001) Oxidation of active center cysteine of bovine 1-Cys peroxiredoxin to the cysteine sulfenic acid form by peroxide and peroxynitrite. *Free Radical Biol. Med. 31*, 292–303.

(34) Jaschke, A., Mi, H., and Tropschug, M. (1998) Human T cell cyclophilin18 binds to thiol-specific antioxidant protein Aop1 and stimulates its activity. *J. Mol. Biol. 277*, 763–769.

(35) Lee, S. P., Hwang, Y. S., Kim, Y. J., Kwon, K. S., Kim, H. J., Kim, K., and Chae, H. Z. (2001) Cyclophilin a binds to peroxiredoxins and activates its peroxidase activity. *J. Biol. Chem. 276*, 29826–29832.

(36) Laxa, M., Konig, J., Dietz, K. J., and Kandlbinder, A. (2007) Role of the cysteine residues in *Arabidopsis thaliana* cyclophilin CYP20-3 in peptidyl-prolyl cis-trans isomerase and redox-related functions. *Biochem. J. 401*, 287–297.

(37) De Simoni, S., Goemaere, J., and Knoops, B. (2008) Silencing of peroxiredoxin 3 and peroxiredoxin 5 reveals the role of mitochondrial peroxiredoxins in the protection of human neuroblastoma SH-SY5Y cells toward MPP+. *Neurosci. Lett. 433*, 219–224.

(38) Trujillo, M., Clippe, A., Manta, B., Ferrer-Sueta, G., Smeets, A., Declercq, J. P., Knoops, B., and Radi, R. (2007) Pre-steady state kinetic characterization of human peroxiredoxin 5: taking advantage of Trp84 fluorescence increase upon oxidation. *Arch. Biochem. Biophys. 467*, 95–106.

(39) Cadenas, E. (2004) Mitochondrial free radical production and cell signaling. *Mol. Aspects Med. 25*, 17–26.

(40) Watabe, S., Hiroi, T., Yamamoto, Y., Fujioka, Y., Hasegawa, H., Yago, N., and Takahashi, S. Y. (1997) SP-22 is a thioredoxin-dependent peroxide reductase in mitochondria. *Eur. J. Biochem. 249*, 52–60.